A SYSTEMATIC MEASUREMENT OF THE MASS-LOSS RATE OF ζ ORI

1 Measuring the mass-loss rates of O stars

The radiatively driven winds of massive stars are a major source of mechanical and chemical feedback into the ISM, and the mass loss has a crucial role in the evolution of the stars themselves. The key quantity which determines their impact is the mass-loss rate (Puls et al., 2008). A little over a decade ago, mass-loss rates of O stars were thought to be well-measured (e.g., Puls et al., 1996), but recent work has shown that mass-loss rates have likely been overestimated by factors of a few up to an order of magnitude.

There are several well-established diagnostics of mass loss, but all of them suffer from uncertainties that result from the complex structure of stellar winds. At the simplest level, the inhomogeneity of the winds leads to increased emission from two-body processes such as Hα recombination and radio free-free emission. Furthermore, the degree of inhomogeneity may be a function of radius, so that diagnostics originating in different parts of the wind are differently affected (Puls et al., 2006). P Cygni UV absorption line profiles provide further powerful diagnostics, and a large body of work has emerged that suggests that mass-loss rates derived from recombination lines and radio emission are too high by a factor of a few up to over an order of magnitude (e.g., Bouret et al., 2005; Fullerton et al., 2006). Recent work suggests that non-monotonic velocity fields are important in evaluating UV line profiles, and accounting for them reduces the magnitude of the discrepancy (Sundqvist et al., 2010).

In the last decade, observations with the *Chandra* HETGS and XMM-*Newton* RGS have begun to provide additional strong constraints on mass-loss rates of bright Galactic O stars. The primary diagnostics are the shapes of X-ray emission line profiles, which probe the optical depth of the wind and are insensitive to clumping and ionization balance. Extracting mass-loss rates from X-ray line profiles requires careful modeling, as well as data of high statistical quality.

We propose to measure the mass-loss rate of the O supergiant ζ Orionis using a robust, new technique based on precise measurements of the resolved, asymmetric X-ray emission line profile shapes. Because this measurement is a direct probe of the effective wind column density, it is a necessary complement to the diagnostics used in other wavelength bands.

2 X-ray mass-loss diagnostics

2.1 Mechanisms for X-ray emission from massive stars

O-star winds are driven by scattering of radiation in spectral lines. This force is known to be subject to strong instabilities. Numerical hydrodynamic simulations of the winds have led to a picture in which dense clumps of gas form in the wind, while thin streams of gas are accelerated into them, forming strong shocks and heating the gas to X-ray emitting temperatures of a few million Kelvin (MK) (Owocki et al., 1988; Feldmeier et al., 1997).

It is known that in a few exciting cases anomalously bright and hot X-ray emission results from another mechanism (e.g. the magnetically channeled wind of θ^1 Ori C, or the colliding wind emission from evolved massive binaries). However, the line driving instability mechanism appears to be responsible for the X-ray emission from many "normal" O stars such as ζ Pup (Kahn et al., 2001; Cassinelli et al., 2001; Kramer et al., 2003) and ζ Ori (Cohen et al., 2006). The most important pieces of evidence supporting this case are the Doppler widths of the emission lines, which are of order the wind terminal velocity; the f/i ratios of He-like lines, which indicate formation radii in the winds (Leutenegger et al., 2006); and the temperatures ($\sim 1-5$ MK), which are much lower than temperatures observed from magnetically chanelled winds or colliding wind binaries ($\sim$ tens of MK). Note that Bouret et al. (2008) have recently detected a weak magnetic field on ζ Ori, but they have concluded that the

field strength is too low to significantly affect the wind structure or X-ray emission.

2.2 Dependence of profile shape on wind optical depth

O star winds are typically moderately opaque to X-rays, with the microscopic opacity depending on wavelength. This opacity leads to asymmetry in the shape of the resolved emission line profiles, since the redshifted emission from the back hemisphere is more absorbed than the blueshifted emission from the front hemisphere (Owocki & Cohen, 2001).

In Figure 1 we show model line profiles illustrating the effect of characteristic wind optical depth on profile asymmetry. The characteristic wind optical depth is defined as $\tau_* \equiv \kappa(\lambda)\dot{M}/4\pi R_* v_\infty$, where κ is the atomic opacity of the wind, $\dot{M}$ is the stellar mass-loss rate, R_* is the stellar radius, and v_∞ is the wind terminal speed. **The degree of profile asymmetry increases with increasing τ_*.**

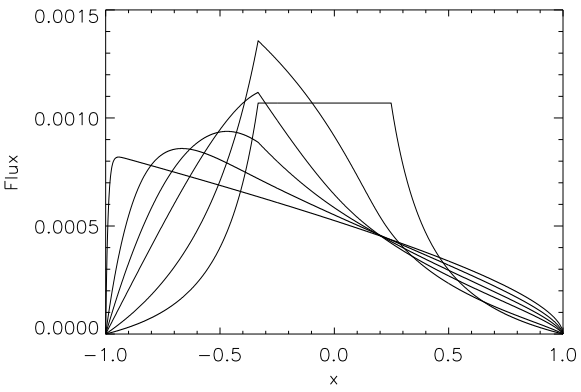

Figure 1: Model line profiles for a non-porous wind; x is the Doppler shift scaled by the wind terminal velocity. The profiles have wind optical depth $\tau_* = 0,\ 1,\ 3,\ 5,\ 10,\ 100$, from most symmetric to most skewed.

Early high resolution *Chandra* and XMM spectra of O stars showed empirical evidence for less profile asymmetry than expected from mass-loss rates inferred from Hα and radio emission, and subsequent quantitative studies of line profiles have confirmed this (Kramer et al., 2003; Oskinova et al., 2006; Cohen et al., 2006, 2010). The moderate asymmetry of the profiles suggests that mass-loss rate reductions are necessary.

2.3 Measuring the mass-loss rate and testing porosity using an ensemble of lines

However, there is an alternative physical explanation for the moderate asymmetry observed in O-star X-ray line profiles: the wind absorption may be reduced if the winds are not only clumpy, but also *porous* (Oskinova et al., 2006; Owocki & Cohen, 2006). A porous wind is a special case of a clumpy wind where the clumps are geometrically large enough for light to propagate between them. This condition is satisified if the *porosity length* $h \equiv l f_{cl}$ is at least of order the stellar radius. Here l is the clump size and f_{cl} is the clumping factor. Thus, for typical clumping factors ~ 10, the clump size must be $\gtrsim 0.1 R_*$ for the wind to be porous. Although this is not impossible, typical clump sizes in numerical hydrodynamic simulations are much smaller (Owocki & Cohen, 2006), and there is no empirical evidence suggesting that clumps this large exist.

Porous winds produce X-ray profiles which are more symmetric than non-porous winds, given the same mass-loss rate. Thus, it is qualitatively possible to explain the moderate asymmetry of X-ray line profiles with a porous model with little or no reduction in mass-loss rate. Porous and non-porous line profiles are quantitatively distinguishable, although ruling out porosity as an important effect using profile shapes typically requires high signal-to-noise profile data (Cohen et al., 2007).

By using all observable X-ray emission lines in a spectrum, we have a means to easily test the importance of porosity in line profile formation. **A strongly porous wind has opacity determined purely by its geometry, and is thus grey, while a non-porous wind has a strongly wavelength dependent opacity determined by the atomic opacity.** Intermediate porosity regimes are non-grey, but the run of effective wind optical depth with wave-

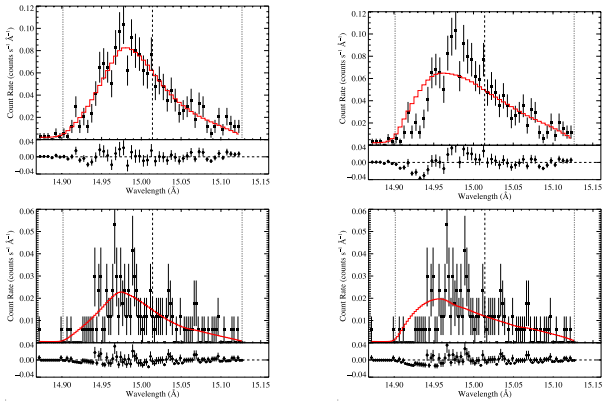

Figure 2: Fe XVII 15.014 Å line in the HETGS spectrum of ζ Pup, with MEG data in the upper panels and HEG data in the lower. The left panels show the best fit model ($\tau_* = 2$), while the right panels show a strongly excluded model with $\tau_* = 5.3$, corresponding to the mass-loss rate inferred from the radio data.

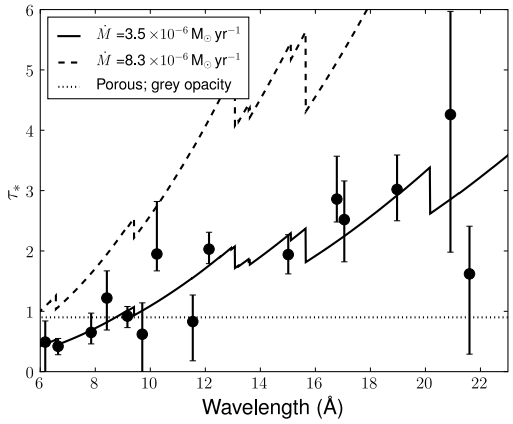

Figure 3: Measured wind optical depth τ_* for ζ Pup, along with several models (Cohen et al., 2010). A constant optical depth is strongly excluded, showing that strong porosity cannot explain the observed X-ray profile shapes.

length is more grey than for a non-porous wind.

We have measured the wavelength dependence of the optical depth of all 16 usable emission lines in the 69 ks *Chandra* HETGS spectrum of ζ Puppis (Cohen et al., 2010); for an example of fits to one strong line, see Figure 2. In Figure 3, we plot the τ_* values derived from fitting each line (points) along with several models of the the expected distribution of τ_* with wavelength (lines). The model optical depths are computed using $\tau_* = \kappa(\lambda)\dot{M}/4\pi v_\infty R_*$, with the model opacity computed using XCMFGEN (described in the next section), and with the mass-loss rate as the only free parameter. The profiles are fit under the assumption of negligible porosity.

In fitting the spectrum of ζ Pup, we have also included the radial dependence of the stellar UV field, which influences the shapes and strengths of the Helium-like forbidden and intercombination lines (Leutenegger et al., 2006). We obtained good fits to the He-like triplets with no additional free parameters, and thus have an independent constraint on the radial location of the X-ray emitting plasma. Combining this with all of the profile fits, we find that the entire X-ray spectrum of ζ Pup can be modeled by a single radial emissivity distribution.

Because we can measure the wind optical depth precisely for a large ensemble of lines, **we are able to constrain $\dot{M}$ to better than 10%** (statistical). The dominant contribution to the uncertainty in our mass-loss rate determination comes from the metallicity.

Furthermore, **we are able to exclude a grey opacity at a high level of confidence, and thus empirically exclude a strongly porous wind for ζ Pup.** An important outstanding question remains: do the results shown in Figure 3 hold for other O stars as well?

3 Global modeling

In addition to the technique of modeling an ensemble of individual line profiles, our group has also developed XCMFGEN, a powerful new tool for global modeling (Zsargó et al., 2008, Zsargo et al. 2010, in preparation). CMFGEN is a code for modeling NLTE radiative transfer in massive star winds; dozens of papers have been published based on spectral modeling with CMFGEN. CMFGEN already includes the effect of X-ray photoionization on the ion balance of the wind; XCMFGEN is an extension of CMFGEN to predict the emergent X-ray emission, which is modeled with APEC, the widely used code

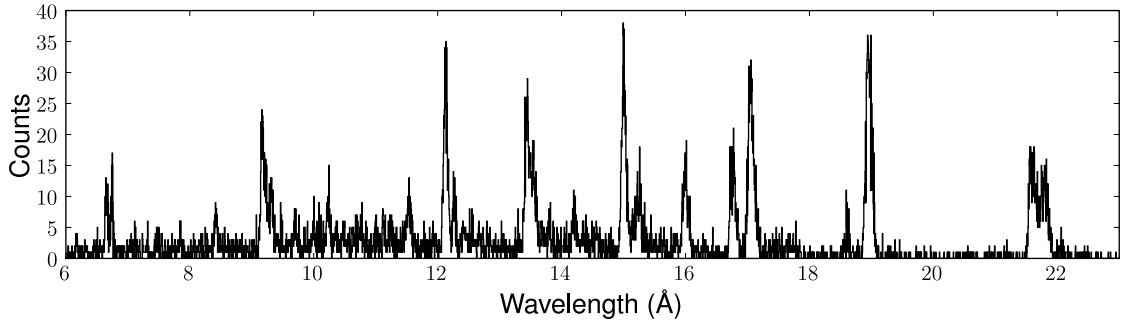

Figure 4: Archival MEG spectrum of ζ Ori, obtained with $\sim$ 74 ks exposure.

for modeling X-ray emission from plasmas in the coronal approximation.

Using XCMFGEN, it is possible to construct a global model that can be simultaneously compared to radio, IR, optical, UV and X-ray data, giving an unprecedented degree of leverage in studies of stellar winds and measurements of their basic parameters.

The accuracy of the model mass-loss rate derived from the X-ray data depends on having an accurate atomic opacity for the wind, which means that we must measure metal abundances as accurately as possible. Measuring these quantities accurately requires XCMFGEN modeling of all available X-ray, UV, and optical data.

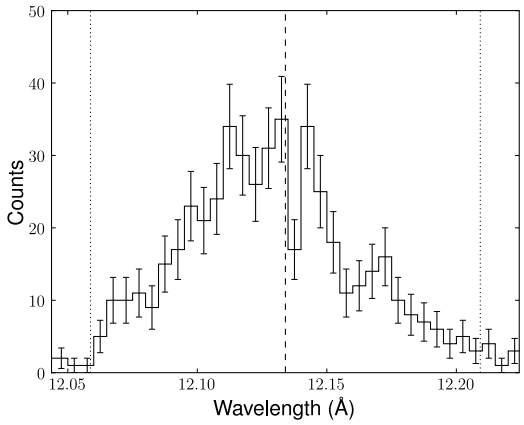

Figure 5: Profile of Ne X Lyα in the archival spectrum of ζ Ori. It is clearly asymmetric, but our ability to extract information is limited by the moderate statistical quality.

4 Archival data of ζ Ori

We show the archival 74 ks MEG spectrum of ζ Ori in Figure 4. There are bright emission lines in the wavelength range 6-23 Å. In Figure 5 we show the observed Ne X Lyα profile from the same spectrum. There is clear evidence for asymmetry, but the statistical quality of the data is only moderate.

In Figure 6 we show our analysis of the archival HETGS spectrum of ζ Ori, using the same methods as Cohen et al. (2010). The points with error bars show measured wind opacities, and the two lines show the model optical depths for two possible values of the mass-loss rate; the red line corresponds to a mass-loss rate of $3.33 \times 10^{-7}\,M_\odot\,yr^{-1}$, while the blue line corresponds to twice that value. We are not able to exclude a grey opacity with the archival data, although it is not favored.

We have also anlayzed the archival XMM-*Newton* RGS spectra of ζ Ori, comprising a total of 137 ks of exposure. We find that the RGS spectra can provide strong constraints on the profile shapes of O Ly α and longer wavelength lines. However, because of the higher spectral resolution of the HETGS, it has an enormous advantage over the RGS in measurement of profile asymmetry at short wavelengths, and at wavelengths shorter than 14Å, it has a much larger effective area as well.

Because ζ Ori has a lower mass-loss rate

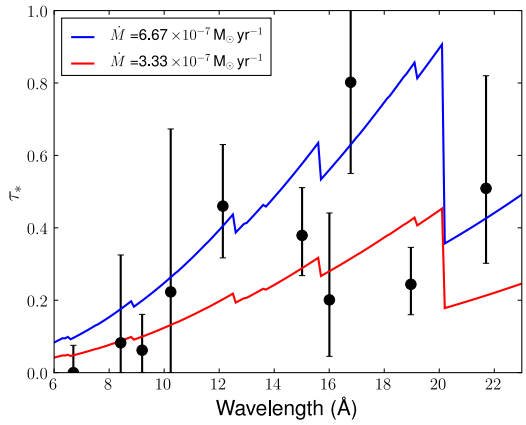

Figure 6: Measured values of τ_* using the archival HETGS spectrum of ζ Ori, shown with two model wind optical depths.

than ζ Pup, the measured wind optical depths are lower as well, and the relative errors are correspondingly higher. It is thus necessary to obtain high signal-to-noise, high spectral resolution line profile measurements in order to test the porosity hypothesis and measure the mass-loss rate as precisely as we have for ζ Pup. The archival HETGS data have insufficient signal-to-noise, and the archival RGS data have insufficient spectral resolving power. Only a long observation with the HETGS can provide the high quality data necessary for our goals of measuring the mass-loss rate and testing the porosity hypothesis.

5 Proposed observation

We propose to reobserve ζ Ori with the HETGS for an additional 300 ks, bringing the total exposure to 374 ks. This will substantially increase the signal-to-noise ratio of the line profiles and much more strongly constrain model parameters. We will apply the same analysis methods as Cohen et al. (2010) to this high-quality data, and we will measure the mass-loss rate while we also test the importance of porosity. We will also leverage the archival RGS data to provide strong constraints on long wavelength lines. However, **only the HETGS can provide the needed spectral resolution** to acheive the goals of this proposal.

In our analysis of ζ Pup, we found that the dominant uncertainty in our mass-loss rate determination was not statistical error on the line profile fits, but systematic uncertainty in the metallicity, through its effect on the opacity. Because of this, we set a goal of a statistical uncertainty of 10% on the derived mass-loss rate.

In Figure 7 we show a simulation of a model Ne X Lyα profile in a 374 ks observation (74 ks archival data plus 300 ks new observations). The simulation are of high statistical quality and strongly constrain the model wind opacity.

We have simulated line profiles from strong lines spanning the observable spectrum of ζ Ori. For each line, we have fit the simulated data with a profile model to obtain simulated measurements of the wind optical depth τ_*. In Figure 8 we show the expected precision we will achieve in measuring τ_* for this ensemble of strong lines; each set of simulated data points would allow us to make a precise measurement of the mass-loss rate of ζ Ori. Using only the simulated measurements of τ_*, the blue points would give a measured mass-loss rate of 7.5 ± 0.5 (in units of $10^{-7}\,M_\odot\,yr^{-1}$), compared with a "true" value of 6.7; and the red points would give a measured mass-loss rate of 2.8 ± 0.3, compared with a "true" value of 3.3. Furthermore, **the new data will distinguish definitively between a grey opacity and a wavelength dependent opacity, and thus will determine whether strong porosity is important in the X-ray emission of ζ Ori**.

Finally, we will generate global models for ζ Ori using XCMFGEN and fit them to the X-ray, UV, optical, and radio observations. Our state of the art modeling capability will allow us to understand the physics of the wind in detail, and to make precise measurements of its fundamental parameters. We will use archival Copernicus, IUE, and GHRS data as well as optical observations of ζ Ori. **Our global modeling with XCMFGEN will strongly constrain elemental abundances and metallicity, and thus X-ray opacity, minimizing the systematic uncertainty in the mass-loss rate**

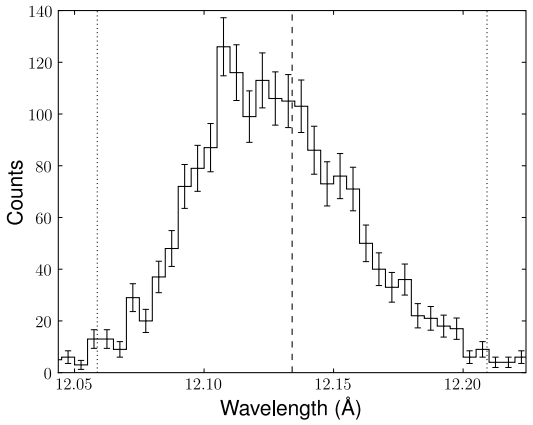

Figure 7: Simulation of the Ne X Lyα profile expected from a 374 ks observation (74 ks archival plus 300 ks new observations). The high statistical quality of the data will enable us to make precise measurements of the profile shape and constrain the wind optical depth.

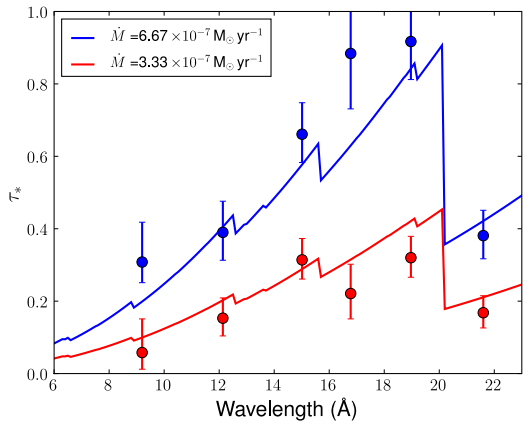

Figure 8: The two lines indicate non-porous model wind optical depths for two possible values of the stellar mass-loss rate, as in Figure 6. The data points are from fits to simulated data based on the model opacities.

determination.

6 Technical Feasibility

The zero order count rate of ζ Ori A is 0.17 s^{-1}, and the effects of pileup on the zero order data will be moderate. The dispersed spectrum will not suffer from pileup.

ζ Ori B is about a factor of ten fainter than ζ Ori A, and they are separated by $\sim 2''$. We have indicated a preferred roll angle tolerance which avoids confusion in the dispersed spectra; however, observations at any roll angle will not compromise out science goals.

There are about 80 days when ζ Ori is not observable in 2012. During much of the rest of the year, observation duration may be limited by thermal constraints. This will not affect our science goals. The periods of most favorable roll angle roughly correspond to the periods where the pitch angle allows unrestricted observing.

We note that there is no evidence for strong time variability in X-ray emission from most "normal" O stars, including in any archival observations of ζ Ori, so that the entire cumulative exposure may be coadded and fit simultaneously.

References

Bouret, J.-C., et al. 2008, MNRAS, 389, 75

Bouret, J.-C., Lanz, T., & Hillier, D. J. 2005, A&A, 438, 301

Cassinelli, J. P., et al. 2001, ApJ, 554, L55

Cohen, D. H., et al. 2006, MNRAS, 368, 1905

Cohen, D. H., Leutenegger, M. A., & Townsend, R. H. D. 2007, 0712, arXiv:0712.1050

Cohen, D. H., et al. 2010, MNRAS, 405, 2391

Feldmeier, A., Puls, J., & Pauldrach, A. W. A. 1997, A&A, 322, 878

Fullerton, A. W., Massa, D. L., & Prinja, R. K. 2006, ApJ, 637, 1025

Kahn, S. M., et al. 2001, A&A, 365, L312

Kramer, R. H., Cohen, D. H., & Owocki, S. P. 2003, ApJ, 592, 532

Leutenegger, M. A., et al. 2006, ApJ, 650, 1096

Oskinova, L. M., Feldmeier, A., & Hamann, W.-R. 2006, MNRAS, 372, 313

Owocki, S. P., Castor, J. I., & Rybicki, G. B. 1988, ApJ, 335, 914

Owocki, S. P. & Cohen, D. H. 2001, ApJ, 559, 1108

—. 2006, ApJ, 648, 565

Puls, J., et al. 1996, A&A, 305, 171

Puls, J., et al. 2006, A&A, 454, 625

Puls, J., Vink, J. S., & Najarro, F. 2008, A&A Rev., 16, 209

Sundqvist, J. O., Puls, J., & Feldmeier, A. 2010, A&A, 510, A11

Zsargó, J., et al. 2008, ApJ, 685, L149

7 Previous Chandra Programs

AO12 - Observation of η Car (co-I) - PI M. Corcoran - Observation scheduled

AO11 - archive (co-I) - PI J. Zsargó - Paper in preparation

AO8 - archive (co-I) - PI D. Cohen - "A Mass-Loss Rate Determination for ζ Puppis from the Quantitative Analysis of X-ray Emission Line Profiles," Cohen et al., 2010 MNRAS 405 2391

AO4 Observation of μ Lep - (co-I) - PI E. Behar - "Resolving X-Ray Sources from B Stars Spectroscopically: The Example of μ Leporis," Behar et al., 2004 ApJ 612 65

Maurice A. Leutenegger Biographical Sketch

EDUCATION

Columbia University, Ph. D., Physics, September 2006, "High Resolution X-ray Spectroscopy of Massive Stars", advisors Frits B. S. Paerels and Steven M. Kahn; M. Phil., Physics, 2000; M. A., Physics, 2000

University of Wisconsin, B. S., Physics, 1998

EMPLOYMENT

Research Associate, NASA/GSFC/CRESST/UMBC, Nov 2010-present

NASA Postdoctoral Fellow, NASA/GSFC, Nov 2007-Nov 2010

Postdoctoral Scientist, Swarthmore College, Fall 2007

Postdoctoral Scientist, Columbia University, 2006-2007

RESEARCH INTERESTS

High resolution X-ray spectroscopy of astrophysical and laboratory plasmas

Instrumentation for X-ray spectroscopy; X-ray calorimeters

Atomic processes in plasmas; charge exchange; laboratory astrophysics

Observations and theory of stellar winds

SELECTED PUBLICATIONS

Leutenegger, M. A.; Cohen, D. H.; Zsargo, J.; Martell, E. M.; MacArthur, J. P.; Owocki, S. P.; Gagné, M.; Hillier, D. J.; "Modeling broadband X-ray absorption of massive star winds" 2010 ApJ 719 1767

Cohen, D. H.; Leutenegger, M. A.; Wollman, E. E.; Zsargo, J.; Hillier, D. J.; Townsend, R. H. D.; Owocki, S. P.; "A mass-loss rate determination for ζ Puppis from the quantitative analysis of X-ray emission line profiles" 2010 MNRAS 405 2391

Zsargó, J.; Hillier, D. J.; Bouret, J.-C.; Lanz, T.; Leutenegger, M. A.; Cohen, D. H.; "On the Importance of the Interclump Medium for Superionization: O VI Formation in the Wind of ζ Puppis" 2008 ApJ 685 149

Leutenegger, M. A.; Owocki, S. P.; Kahn, S. M.; Paerels, F. B. S.; "Evidence for the importance of resonance scattering in the X-ray emission line profiles of the O star ζ Puppis" 2007 ApJ 659 642

Leutenegger, M. A.; Paerels, F. B. S.; Kahn, S. M.; Cohen, D. H.; "Measurements and analysis of helium-like triplet ratios in the X-ray spectra of O stars" 2006 ApJ 650 1096

Cohen, D. H.; Leutenegger, M. A.; Grizzard, K. T.; Reed, C. L.; Kramer, R. H.; Owocki, S. P.; "Wind signatures in the X-ray emission-line profiles of the late-O supergiant ζ Orionis" 2006 MNRAS 368 1905